Journal of Neuropathology and Experimental Neurology

Vol. 57, No. 10
October, 1998
pp. 972–978

Neuropil Threads are Collinear With MAP2 Immunostaining in Neuronal Dendrites of Alzheimer Brain

J. Wesson Ashford MD, PhD, Natalie S. Soultanian PhD, Shu-Xin Zhang MD, PhD, and James W. Geddes PhD

Abstract. Alzheimer disease (AD) neuropathology includes neuropil threads (NTs) and neurofibrillary tangles (NFTs). In tangle-bearing neurons, the normal cytoskeleton is severely disrupted and replaced with paired helical filament (PHF) aggregates of aberrantly phosphorylated microtubule-associated protein tau. In this study, double-label immunocytochemistry was used to clarify the relationship between the appearance of neurofibrillary pathology (NTs and NFTs) and the loss of normal cytoskeletal components, such as microtubule-associated protein 2 (MAP2) in 13 AD cases and 6 nondemented elderly control individuals. Brain areas examined included neocortex (cingulate, motor, and inferior parietal cortices), hippocampus, and entorhinal cortex. In mildly affected neurons, PHF-1 immunostained NTs were found in dendrites, frequently at dendritic branch points, and were adjacent to MAP2 immunostaining. In more severely affected neurons, the PHF-1 immunoreactivity occupied distinct dendritic segments and appeared to displace MAP2. Interspersed MAP2 immunopositive dendritic segments were often beaded in appearance. In all instances where dendrites with NTs could be traced back to the soma, the soma also contained PHF-1 immunostained fibrils in various stages of NFT formation. The results suggest that PHFs gradually displace normal microtubules in dendrites, and cause degeneration of dendritic segments between NTs.

Key Words: Alzheimer disease; Cytoskeleton; Neurodegeneration; Paired helical filaments; Tau.

INTRODUCTION

Alzheimer Disease (AD) is characterized by the presence of several neuropathological structures including neurofibrillary tangles (NFT), senile plaques (SPs), and neuropil threads (NTs), also known as curly fibers. In contrast to the mention of NFTs and SPs in the initial description of AD in 1907 (1, 2), NTs were first noted in 1970 (3) and are now recognized as an extensive and common pathological component of AD (4, 5). NTs are 5–30 μm long, from 0.2 to 1.5 μm in diameter (6, 7). Ultrastructural studies show that NTs consist of straight filaments (8), paired helical filaments (PHFs) (9), or both straight filaments and PHFs (10). Anatomical studies suggest that curly NTs usually appear in the neighborhood of NFTs and SPs (4, 6, 11–13). It is unsettled whether NTs occur exclusively in dendrites (7, 11), or are present in both axons and dendrites (9, 10, 14).

Although NTs are often found near NFTs, few NT-containing processes can be traced back to tangle-bearing neurons or to neurons without NFTs (14). To explore the relationship between NFTs and NTs, Braak et al (13) examined the transentorhinal/entorhinal region in cases without neurofibrillary changes or with only mild alterations. Using the AT8 antibody against phosphorylated tau (15) and Gallyas silver stain method (16), Braak et al characterized 5 stages of neuronal alterations in these cases without neurofibrillary pathology in the surrounding tissue. In Group 1 neurons, granular AT8 immunoreactive material appears to fill the soma, dendrites, and axon. However, these neurons do not exhibit neurofibrillary changes in silver stained sections. Group 2 neurons possess rod-like inclusions in thickened portions of distal dendrites and in the soma. Silver stains also reveal these inclusions. In Group 3 neurons, there are more pronounced alterations in distal dendrites, intermediate dendrites lose immunoreactivity, and the soma is more homogeneously stained. Group 4 structures represent early ghost tangles characterized by course accumulations of AT8-immunopositive granules. Late ghost tangles (group 5 structures) are devoid of AT8 immunoreactivity.

It is not known if a similar progression of neurofibrillary changes occurs in individuals with more advanced pathology. This is difficult to determine, as the increased number of NTs in areas affected by AD makes it troublesome to trace NTs back to individual neurons. It is also unclear if the alterations in tau phosphorylation represent an early or late stage in the cytoskeletal disruption associated with neurofibrillary pathology. Although tau hyperphosphorylation is hypothesized to be a seminal event in PHF formation (17), it is also possible that the tau phosphorylation occurs at relatively late stages of cytoskeletal disruption and PHF formation (18). In 2 previous studies, phosphorylated tau immunoreactivity was compared with that of microtubule-associated protein 2 (MAP2), a somatodendritic cytoskeletal protein. McKee et al (19) reported that most tangle bearing neurons do not contain MAP2, although occasional neurons were observed in which NFTs appeared to push aside the MAP2 reaction product. Lee et al (20) observed that NTs were devoid of MAP2 immunoreactivity.

The purpose of this study was to examine the relationship between alterations in tau phosphorylation and the

From the Sanders-Brown Center on Aging, University of Kentucky, Lexington, Kentucky.

Correspondence to: James W. Geddes, PhD, or J. Wesson Ashford, MD, Sanders-Brown Center on Aging, University of Kentucky, 800 S. Limestone, Lexington, KY 40536-0230.

TABLE
Autopsy Cases Examined

Case	Diagnosis	Age (years)	Gender	Postmortem interval (hours)	Duration of illness (years)	Other conditions
1	AD	76	M	3.57	NA	
2	AD	74	M	2.67	12	
3	AD	79	F	3.33	7	
4	AD	74	M	12.6	14	
5	AD	67	M	3.30	5	
6	AD	83	M	1.55	4	
7	AD	76	F	2.00	11	
8	AD	85	M	4.25	15	
9	AD	81	F	4.25	3	
10	AD	82	M	2.25	9	DLBD
11	AD	75	M	1.92	NA	DLBD
12	AD	80	M	3.08	11	DLBD
13	AD	76	M	4.25	11	
14	C	66	M	2.25		ALS
15	C	79	F	2.00		
16	C	84	F	5.75		
17	C	71	M	3.50		
18	C	95	F	2.17		AD type changes
19	C	79	M	2.12		AD type changes

Abbreviations: AD, Alzheimer disease; ALS, amyotrophic lateral sclerosis; C, nondemented control; DLBD, diffuse Lewy body disease.

loss of MAP2 immunoreactivity in NTs and NFTs. Neurofibrillary changes were examined in individuals with advanced AD, as well as in cases with minimal pathology. Phosphorylated tau was visualized using the PHF-1 antibody (21). Disruption of normal microtubules was assessed by examining MAP2 immunoreactivity, using the monoclonal AP-18 antibody (22). The results indicate that in neurons with both PHF-1 and MAP2 immunoreactivity, NTs occurred as segments collinearly associated with MAP-2. There appeared to be a predilection for NTs to develop at dendritic branch points, even at some distance from the neuronal soma. In neurons with more pronounced NTs, MAP2 in the interspersed dendritic segments often had a beaded, degenerative appearance. These results suggest that the appearance of NTs precedes the loss of MAP2 during neurofibrillary degeneration.

MATERIAL AND METHODS

Cases

Brains of 13 patients with a clinical history of progressive dementia and a neuropathologic confirmation of AD (23) and 6 individuals without dementia were obtained through the autopsy program of the Alzheimer Disease Research Center at the Sanders-Brown Center on Aging of the University of Kentucky (Table). Autopsy cases with short postmortem intervals were utilized, as loss of MAP2 immunoreactivity is evident with long postmortem intervals in the absence of disease (24). The postmortem interval averaged 3.8 ± 0.8 hours (h) for the AD cases, and 3.0 ± 0.6 h for controls (mean ± SEM). The average age of the AD cases was 78 ± 1.3 years, while that of the control group was 79 ± 4.1 years. In addition to the AD pathology, 3 of the AD cases had diffuse Lewy bodies. Mild AD-related neuropathology was present in 2 of the control cases, but was not sufficient to meet the diagnostic criteria for AD.

At autopsy, blocks of brain tissue were removed and fixed in 4% paraformaldehyde (pH 7.4) for approximately 48 h, cryoprotected in 30% sucrose, frozen in powdered dry ice, and then stored at −70°C until required. Blocks of brain tissue (posterior cingulate cortex, anterior cingulate cortex, hippocampus, entorhinal cortex, superior temporal cortex, inferior parietal cortex, and motor cortex) were cut (30 μm thickness) on a freezing microtome (Zeiss).

Immunocytochemistry

For immunocytochemical staining of NFTs and NTs, the PHF-1 monoclonal antibody was used (21, 25). This antibody was chosen because of its specificity for tangle-related changes in tau phosphorylation (13, 25). PHF-1 recognizes tau phosphorylated at serine residues 396 and 404 (22). The AP-18 mouse monoclonal antibody was used for detection of MAP2. This antibody recognizes both the high and low molecular weight MAP2 isoforms (17).

The tissue sections were processed "free-floating" using 24 well culture plates, 1 section per well. Following 3 rinses in Tris-buffered saline (TBS, 50 mM, pH 7.4), endogenous peroxidase activity was blocked using 3% hydrogen peroxide in TBS for 10 minutes (min). Sections were transferred to TBS containing 1% Triton-X-100 (Tris-A), followed by incubation in Tris-A containing 1.5% normal horse serum. Sections were then incubated in the primary antibody PHF-1 (1:1000) or AP-18 (1:10,000) overnight at room temperature. After 3 rinses in Tris-A, immunostaining was performed using a biotinylated

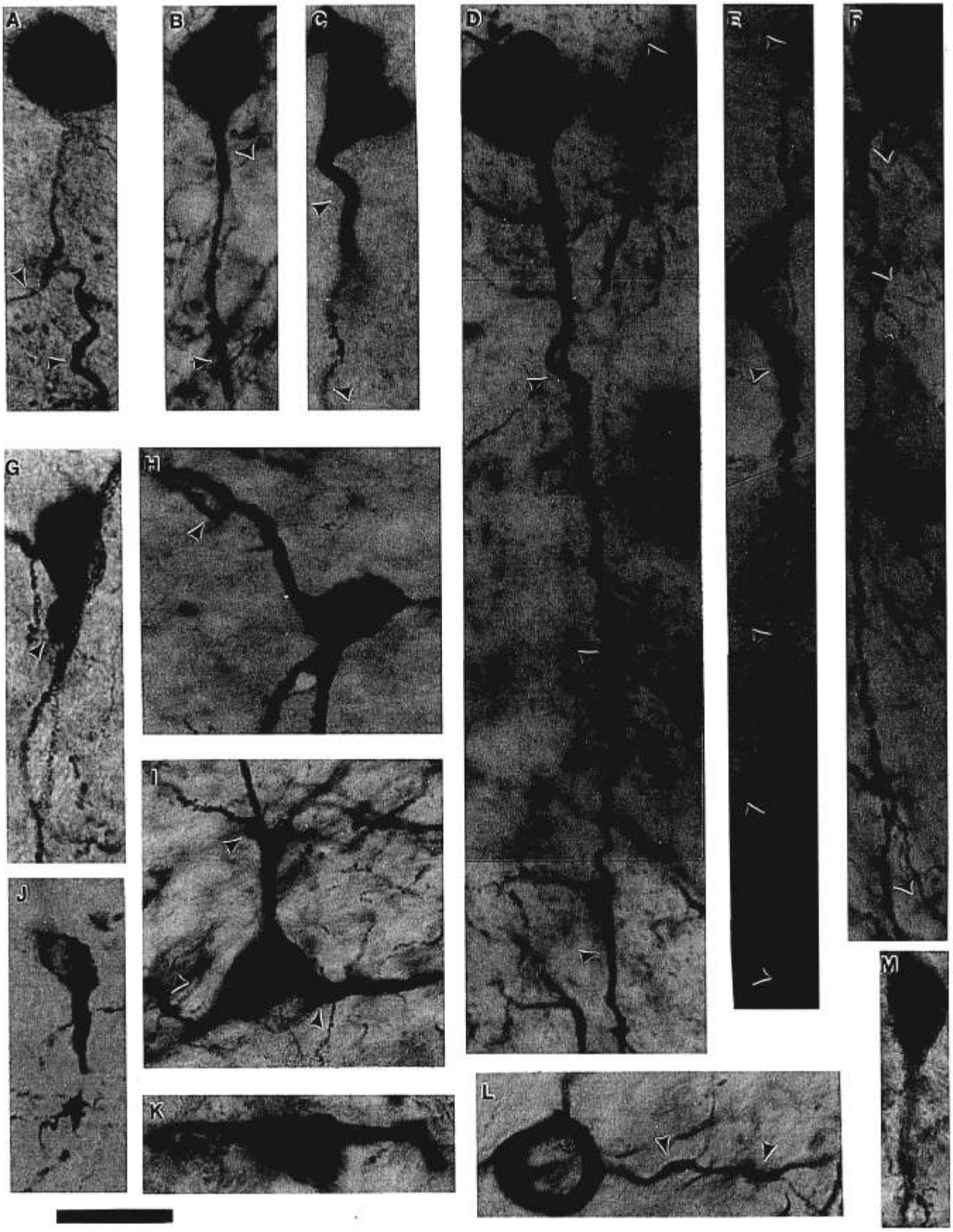
A
B
C
D
E
F
G
H
I
J
K
L
M

anti-mouse secondary antibody preabsorbed against rat serum (1:200; Vector) and streptavidin peroxidase (1:500; Zymed). The peroxidase substrate used was 3,3'-Diaminobenzidine (DAB, Sigma).

For double-immunolabeling, sections were processed for the first primary antibody (PHF-1, 1:1000), as described above using DAB (brown stain) as a first chromogen. Following several rinses in TBS and an additional blocking step, the sections were incubated in the second primary antibody (AP-18, 1:10,000) overnight at room temperature. Immunostaining was performed as described above, but 4-Chloro-1-Naphthol (Sigma, dark purplish stain) or Pyronin B (Sigma, pink stain) were used as the peroxidase substrate.

To determine the specificity of the procedure, in some experiments double-label immunocytochemistry was performed using alkaline phosphatase (Elite Alkaline Phosphatase kit, Vector Laboratories) instead of streptavidin peroxidase and Vector Red (Vector laboratories) as a substrate for 1 antibody. The results obtained were similar to those observed using peroxidase substrates. Negative controls consisted of omission of first or second primary antibodies (partial omission); omission of both primary antibodies (total omission); substitution of mouse IgG 2A for either or both primary antibodies; replacement of the biotinylated anti-mouse secondary antibody with an inappropriate biotinylated anti-rabbit antibody; and preabsorbtion of primary antibodies with excess antigen.

RESULTS

MAP-2 immunostaining was present in the soma and dendrites of neurons of both AD patients and controls. In controls, the AP-18 immunopositive dendrites showed very few disruptions (Fig. 1M), and those present were 1–3 μm in length. In all of the AD patient sections examined in this study, the AP-18 immunopositive dendrites had frequent short gaps (5–25 μm) with a bead-like or broken line appearance which was not observed in the control cases (Fig. 1J).

PHF-1 immunostaining was evident in all examined regions of the brains of the AD patients, although the motor cortex was less affected. Minimal PHF staining was observed in 2 control cases, and had a much more limited distribution.

In double-label immunostained sections, PHF-1 immunoreactivity was often present in the larger gaps in AP-18 immunostained dendrites in AD cases (Fig. 1A–I, L) but was not observed between the small gaps in control cases. In the AD cases, the high density of both PHF-1 and MAP-2 staining in the gray matter made it difficult to follow individual neurons. Single neurons were observed most clearly at the interface between the gray and white matter. In each neuron in which the dendritic PHF-1 immunoreactive segments were observed, the soma also contained PHF-1 immunoreactive fibrils (Fig. 1A–I, K, L). The perikaryal PHF-1 stained inclusions varied in size, ranging from small spindle-shaped structures occupying a small portion of the cell body (Fig. 1E, F, H) to large fibrillary tangles which occupied nearly the full soma (Fig. 1B–D). Similarly shaped PHF-1 immunostained structures were found in extracellular or ghost tangles, where they were not associated with MAP-2 staining (not shown).

The interspersed segments of MAP-2 and PHF-1 staining were detected in several brain regions, with the most numerous occurrences in posterior cingulate cortex, entorhinal cortex, hippocampus, and the inferior parietal cortex. There were only a few segments of interspersed staining in the anterior cingulate cortex, and even fewer in the superior temporal region. PHFs were infrequently observed in the primary motor cortex. Although double-label immunostained neurons were present in both neocortex and hippocampus, the appearance of the staining differed between these regions. In the hippocampus, the double-stained somata frequently had no dendrites, and were often oval-shaped. A similar oval shape was noted for double-stained neurons in the entorhinal cortex, but these cells had more dendrites than the hippocampal cells.

PHF-1 immunostained segments seemed to occur more frequently at branch points (Fig. 1A, B, D, H, I, L) but not exclusively (Fig. 1C–F). There was no indication that the PHF-1 segments occurred closer to or further away from cell bodies, as segments appeared to be present at semiregular intervals along the dendrite (Fig. 1D–F). In some cases, the PHF-1 immunostained segments appeared to have broken out of the dendrite (Fig. 1D). Many of the MAP2 immunostained segments located between the PHF-1 positive NTs appeared to be degenerating, based on their beaded appearance (Fig. 1C, E). The

←

Fig. 1. Double-immunolabeling of posterior cingulate neurons for PHF-1 and MAP2. Diamobenzidine was used as the chromogen for PHF-1 (brown stain); Pyronin B was used as the chromogen for MAP2 (AP-18 antibody, pink-purple stain). Panels A to L are from AD cases: (A, E and F are from Case 12, see Table; C and K from Case 3; H, I, and L from Case 11; B from Case 6; D from Case 1; G from Case 2). The neuron in panel J is stained only with AP-18 (anti-MAP2 monoclonal antibody) and is from Case 3. Panel M is from a nondemented elderly individual (Case 14). PHF-1 immunoreactive segments, indicated by arrowheads, are evident in panels A–K. In some neurons, only small wisps of PHF-1 stained material are evident, primarily at dendritic branch points, and these appear to coexist with MAP2 (H, I, L). In other cases, PHF-1 stained segments occupy entire dendritic regions, and appear to replace MAP2 (A, B, D, E). All neurons with dendritic PHF-1 immunostaining also had somal PHF-1 immunoreactivity. This could occupy small areas of the soma (H) or almost fill the neuronal cell body (B, D, I). Single label MAP2 immunostaining revealed large gaps in the dendrites of AD cases (J) which were not observed in control cases (M). The scale bar at the lower left corner represents 20 μm and applies to all panels.

beading was restricted to the MAP2 immunopositive dendritic segments, and was not observed in the PHF-1 positive regions. The beading was also specific to neurons with neurofibrillary pathology.

In interpreting these results, the methodological limitations of the double staining must also be considered. For example, it is possible that in some cases the MAP2 and PHF-1 immunostained segments were present on adjacent overlapping neurites, rather than in a single neurite (e.g. Fig. 1D, L). However, microscopic examination of individual neurites, in various planes of focus, reinforced the interpretation that the PHF-1 and MAP2 segments were present in the same neurite. It is possible that some of the observed gaps in MAP2 immunostaining were artifacts, due to a plane of section effect. However, the large gaps in MAP2 immunostaining were consistently observed in the AD cases and not in the controls.

DISCUSSION

The purpose of this study was to examine the relationship between alterations in tau phosphorylation and the loss of MAP2 immunoreactivity in NTs and NFTs. If altered tau phosphorylation is an early event in neurofibrillary pathology, changes in tau phosphorylation should be evident prior to the loss of MAP2. Alternatively, tau hyperphosphorylation may be a relatively late event in the sequence of cytoskeletal changes (18). In response to neuronal insults such as focal ischemia and excitotoxic insult, tau is spared relative to MAP2 (26), which is similar to the preservation of tau in AD. However, most insults examined to date result in tau dephosphorylation, in contrast to the hyperphosphorylation observed in AD (27–30). It is possible that tau hyperphosphorylation may be a compensatory response to the neuronal insult and occur after the tau dephosphorylation and loss of MAP2 (18). To distinguish between these possibilities, we examined phosphorylated tau immunoreactivity using the PHF-1 antibody, and MAP2 using the AP18 antibody.

PHF-1 immunoreactivity was evident in dendrites prior to any apparent loss of MAP2. The small fragments of PHF-1 immunoreactive material were often found at dendritic branch points. Tracing the dendrite back to the cell body indicated that the same neurons also had PHF-1 immunoreactive fibrils in the soma. However, it should be noted that Schmidt et al observed occasional NTs that could be traced back to neurons without NFTs (14). As the amount of PHF-1 immunoreactive material in the dendrites increased, MAP2 immunoreactive segments appeared to become displaced. At later stages, the MAP2 positive dendritic segments between PHF-1 stained fragments were often beaded in appearance. Large gaps in MAP2 immunostained dendrites were evident in the AD cases, but not in cases without neurofibrillary pathology. These results suggest that the PHF-1 positive NTs segments are causally related to the dendritic degeneration.

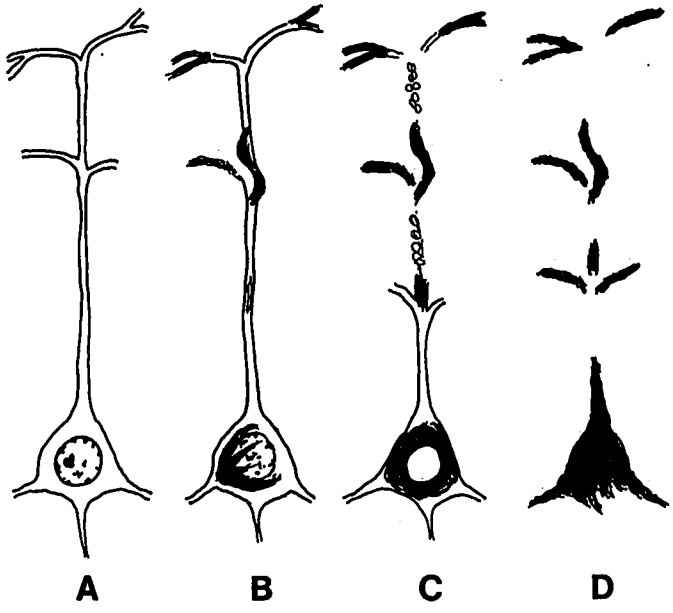

Fig. 2. A schematic representation of the relationship between PHF-1 immunopositive NTs, NFTs, and MAP2 immunostaining. A: normal neuron without NTs or NFTs. B: NTs form in dendrites, particularly at dendritic branch points, simultaneously with the appearance of PHF-1 positive fibrils in the soma. This is an early stage intracellular tangle. C: NTs grow to completely fill the dendritic segment, replacing MAP2 and causing degeneration of intervening dendritic segments. D: Eventually the MAP2-immunopositive dendrites are lost and the soma is filled with the NFT. This represents an extracellular 'ghost' tangle and neuropil threads.

Previous studies indicated that MAP2 is absent from NTs (20) but may be occasionally found in NFTs (20). The results of this study do not suggest that MAP2 is present in NTs, but demonstrate that NTs are adjacent to MAP2 at early stages of NT formation. As the NTs increase in size, MAP2 is lost from the dendritic segment occupied by the NT. Ihara et al (6, 31) suggested that the ends of the NTs may be newly formed processes, and thus represent growing tips of dendrites or newly formed branches. In contrast, the results of this study indicate that NTs can form at several points within a single dendrite, and are associated with degenerative events.

Previously, Braak et al identified a sequence of changes in phosphorylated tau immunoreactivity associated with the progression of neurofibrillary pathology (NFTs and NTs) (13). Their study focused on the transentorhinal cortex in cases with minimal neurofibrillary pathology in other brain regions. The results of the present study suggest that a similar sequence of events occurs in neocortical tissues in cases with AD and extensive neurofibrillary pathology (Fig. 2). The present study utilized the PHF-1 antibody, in contrast to AT8 used by Braak. Although both antibodies recognize phosphorylated tau epitopes (15, 25, 32), PHF-1 is more specific for tangle-related changes in tau immunostaining than is AT8 (33).

In the Group I neurons described by Braak, AT8 immunocytochemical changes were not accompanied by neurofibrillary alterations detected using the Gallyas silver method. These changes were also not evident using the PHF-1 antibody. The neurons containing PHF-1 immunostained segments, collinear with MAP2 positive dendritic segments, are similar to the Group 2 and Group 3 neurons described by Braak (34). Although both studies observed immunoreactivity at dendritic branch points, we did not observe more pronounced changes in the distal parts of dendrites described by Braak. Overall, the progression of changes observed with PHF-1 immunoreactivity in the AD cases in the present study closely resembles that observed by Braak in cases with minimal neurofibrillary pathology. This suggests that similar mechanisms are associated with the development of neurofibrillary pathology at both initial and advanced stages.

The presence of PHF-1 positive NTs at neuritic branch points is consistent with observations by Braak, and also with the localization of Alz-50 and AT8 immunostaining in tangle-bearing neurons in the cerebral cortex of sheep (35). In the sheep, ultrastructural studies indicate that at least some of the Alz-50 immunoreactivity is associated with ribosomes, which are enriched at dendritic branch points (35, 36). This suggests that the Alz-50 staining may represent newly synthesized tau protein. Alternatively, the localization of NTs at dendritic branch points may reflect accumulation of the protein due to a slowing of dendritic transport at the bifurcation. In neurons with minimal neurofibrillary pathology, the perikaryal PHF-1 immunostaining appears to originate from a single point in the cytoplasm (Fig. 1H), or is concentrated at the periphery (Fig. 1L). This is similar to the distribution of newly formed microtubules in cultured sympathetic neurons (37, 38). Microtubules are assembled at the centrosome, released into the cytoplasm, and rapidly transported into axons and dendrites. PHFs could follow a similar route of assembly, release, and transport, resulting in the formation of NFTs in the perikarya and NTs in axons and dendrites.

The beaded appearance of MAP2 between PHF-1 positive dendritic segments resembles the appearance of MAP2 following excitotoxic insult (39) and related conditions such as ischemia (40) and metabolic impairment (29). It is not likely that the MAP2 beading reflects postmortem changes, since similar alterations in MAP2 were not evident in control individuals without neurofibrillary changes, and were not observed in our previous studies of postmortem cytoskeletal alterations (24, 41). It is more likely that the PHF-1 positive dendritic segments disrupt dendritic transport, including delivery of mitochondria to the intervening segments, and thereby enhance vulnerability to insults including postmortem ischemia.

In conclusion, the results of this study support the hypothesis that tau hyperphosphorylation is an early event in the cytoskeletal disruption evident in AD (17, 42). PHF-1 immunopositive fibrils were observed in the soma and dendrites prior to a detectable loss of MAP2 immunostaining. The results further illustrate that the progressive accumulation of NTs in the dendrite plays a causal role in the degeneration of the intervening dendritic segments.

ACKNOWLEDGMENTS

This research was supported by NIH grant P50 AG05144. We thank Dr. L. I. (Skip) Binder for the generous gift of the AP-18 antibody, and Dr. Sharon Greenberg for the generously providing the PHF-1 antibody. We also thank Dr. William Markesbery and Dr. Daron Davis for the excellent neuropathologic evaluation of the autopsy cases examined in this study.

REFERENCES

1. Stelzmann RA, Schnitzlein HN, Murtagh FR. An English translation of Alzheimer's 1907 paper, "Über eine eigenartige Erkankung der Hirnrinde." Clin Anat 1995;8:429–31
2. Jarvik L, Greenson H. About a peculiar disease of the cerebral cortex. By Alois Alzheimer, 1907 (Translation). Alzheimer Dis Assoc Disord 1987;1:3–8
3. Tomlinson BE, Blessed G, Roth M. Observations on the brains of demented old people. J Neurol Sci 1970;11:205–42
4. Braak H, Braak E, Grundke-Iqbal I, Iqbal K. Occurrence of neuropil threads in the senile human brain and in Alzheimer's disease: A third location of paired helical filaments outside of neurofibrillary tangles and neuritic plaques. Neurosci Lett 1986;65:351–55
5. Markesbery WR, Wang HZ, Kowall NW, Kosik KS, McKee AC. Morphometric image analysis of neuropil threads in Alzheimer's disease. Neurobiol Aging 1993;14:303–7
6. Ihara Y. Massive somatodendritic sprouting of cortical neurons in Alzheimer's disease. Brain Res 1988;459:138–44
7. Yamaguchi H, Nakazato Y, Shoji M, Ihara Y, Hirai S. Ultrastructure of the neuropil threads in the Alzheimer brain: Their dendritic origin and accumulation in the senile plaques. Acta Neuropathol (Berl) 1990;80:368–74
8. Onorato M, Mulvihill P, Copnnolly J, Galloway P, Whitehouse P, Perry G. Alteration of neuritic cytoarchitecture in Alzheimer disease. Prog Clin Biol Res 1989;317:781–89
9. Ohtsubo K, Izumiyama N, Kuzuhara S, Mori H, Shimada H. Curly fibers are tau-positive strands in the pre- and post-synaptic neurites, consisting of paired helical filaments: Observations by the freeze-etch and replica method. Acta Neuropathol (Berl) 1990;81:111–15
10. Perry G, Kawai M, Tabaton M, et al. Neuropil threads of Alzheimer's disease show a marked alteration of the normal cytoskeleton. J Neurosci 1991;11:1748–55
11. Braak H, Braak E. Neuropil threads occur in dendrites of tangle-bearing nerve cells. Neuropathol Appl Neurobiol 1988;14:39–44
12. Kowall NW, Kosik KS. Axonal disruption and aberrant localization of tau protein characterize the neuropil pathology of Alzheimer's disease. Ann Neurol 1987;22:639–43
13. Braak E, Braak H, Mandelkow EM. A sequence of cytoskeleton changes related to the formation of neurofibrillary tangles and neuropil threads. Acta Neuropathol (Berl) 1994;87:554–67
14. Schmidt ML, Murray JM, Trojanowski JQ. Continuity of neuropil threads with tangle-bearing and tangle-free neurons in Alzheimer disease cortex. A confocal laser scanning microscopy study. Mol. Chem. Neuropath. 1993;18:299–312
15. Szendrei GI, Lee VM, Otvos L, Jr. Recognition of the minimal epitope of monoclonal antibody Tau-1 depends upon the presence

of a phosphate group but not its location. J Neurosci Res 1993;34: 243–49
16. Gallyas F. Silver staining of Alzheimer's neurofibrillary changes by means of physical development. Acta Morphol Acad Sci Hung 1971;19:1–8
17. Lee VM, Trojanowski JQ. The disordered neuronal cytoskeleton in Alzheimer's disease. Curr Opin Neurobiol 1992;2:653–56
18. Geddes JW, Mattson MP. Tau hyperphosphoryation and free radicals in PHF formation: Early or late events? Neurobiol. Aging 1995;16:399–402
19. McKee AC, Kowall NW, Kosik KS. Microtubular reorganization and dendritic growth response in Alzheimer's disease. Ann Neurol 1989;26:652–59
20. Schmidt ML, Lee VM, Trojanowski JQ. Comparative epitope analysis of neuronal cytoskeletal proteins in Alzheimer's disease senile plaque neurites and neuropil threads. Lab Invest 1991;64:352–57
21. Greenberg SG, Davies P, Schein JD, Binder LI. Hydrofluoric acid-treated tau PHF proteins display the same biochemical properties as normal tau. J Biol Chem 1992;267:564–69
22. Tucker RP, Binder LI, Viereck C, Hemmings B, A., Matus A. The sequential appearance of low- and high-molecular weight forms of MAP 2 in the developing cerebellum. J. Neurosci. 1988;8:4503–12
23. Geddes JW, Tekirian TL, Soultanian NS, Ashford JW, Davis DG, Markesbery WR. Comparison of neuropathologic criteria for the diagnosis of Alzheimer's disease. Neurobiol Aging 1997;18:S99–105
24. Schwab C, Bondada V, Sparks DL, Cahan LD, Geddes JW. Postmortem changes in the levels and localization of microtubule-associated proteins (tau, MAP2 and MAP1B) in the rat and human hippocampus. Hippocampus 1994;4:210–25
25. Otvos L, Jr., Feiner L, Lang E, Szendrei GI, Goedert M, Lee VM. Monoclonal antibody PHF-1 recognizes tau protein phosphorylated at serine residues 396 and 404. J Neurosci Res 1994;39:669–73
26. Pettigrew LC, Holtz ML, Craddock SD, Minger SL, Hall N, Geddes JW. Microtubular proteolysis in focal cerebral ischemia. J Cereb Blood Flow Metab 1996;16:1189–1202
27. Geddes JW, Schwab C, Craddock S, Wilson JL, Pettigrew LC. Alterations in tau immunostaining in the rat hippocampus following transient cerebral ischemia. J Cereb Blood Flow Metab 1994;14: 554–64
28. Geddes JW, Bondada V, Keller JN. Effects of intrahippocampal colchicine administration on the levels and localization of microtubule-associated proteins, tau and MAP2. Brain Res 1994;633:1–8
29. Pang Z, Umberger GH, Geddes JW. Neuronal loss and cytoskeletal disruption following intrahippocampal administration of the metabolic inhibitor malonate: Lack of protection by MK-801. J Neurochem 1996;66:474–84
30. Davis DR, Anderton BH, Brion JP, Reynolds CH, Hanger DP. Oxidative stress induces dephosphorylation of tau in rat brain primary neuronal cultures. J Neurochem 1997;68:1590–97
31. Iwatsubo T, Hasegawa M, Esaki Y, Ihara Y. Lack of ubiquitin immunoreactivities at both ends of neuropil threads. Possible bidirectional growth of neuropil threads. Am J Pathol 1992;140:277–82
32. Goedert M, Jakes R, Vanmechelen E. Monoclonal antibody AT8 recognises tau protein phosphorylated at both serine 202 and threonine 205. Neurosci Lett 1995;189:167–69
33. Kimura T, Ono T, Takamatsu J, et al. Sequential changes of tau-site-specific phosphorylation during development of paired helical filaments. Dementia 1996;7:177–81
34. Braak H, Braak E, Strothjohann M. Abnormally phosphorylated tau protein related to the formation of neurofibrillary tangles and neuropil threads in the cerebral cortex of sheep and goat. Neurosci Lett 1994;171:1–4
35. Nelson PT, Saper CB. Ultrastructure of neurofibrillary tangles in the cerebral cortex of sheep. Neurobiol Aging 1995;16:315–23
36. Peters A, Palay SL, Webster HD. The fine structure of the nervous system. 3rd ed. New York: Oxford University Press, 1991
37. Ahmad FJ, Baas PW. Microtubules released from the neuronal centrosome are transported into the axon. J Cell Sci 1995;108:2761–69
38. Baas PW, Yu W. A composite model for establishing the microtubule arrays of the neuron. Mol Neurobiol 1996;12:145–61
39. Park JS, Bateman MC, Goldberg MP. Rapid alterations in dendrite morphology during sublethal hypoxia or glutamate receptor activation. Neurobiol Dis 1996;3:215–27
40. Matesic DF, Lin RC. Microtubule-associated protein 2 as an early indicator of ischemia-induced neurodegeneration in the gerbil forebrain. J Neurochem 1994;63:1012–20
41. Geddes JW, Bondada V, Tekirian TL, Pang Z, Siman RG. Perikaryal accumulation and proteolysis of neurofilament proteins in the postmortem rat brain. Neurobiol Aging 1995;16:651–60
42. Bancher C, Braak H, Fischer P, Jellinger KA. Neuropathological staging of Alzheimer lesions and intellectual status in Alzheimer's and Parkinson's disease patients. Neurosci Lett 1993;162:179–82

Received May 28, 1998
Revision received July 17, 1998
Accepted July 17, 1998